

In Vivo Fiber-Coupled Pre-Clinical Confocal Laser-scanning Endomicroscopy (pCLE) of Hippocampal Capillaries in Awake Mice

Rocio Leal-Campanario^{1,2}, Susana Martinez-Conde^{2,3}, Stephen L. Macknik^{2,3}

¹ División de Neurociencias, Universidad Pablo de Olavide ² Barrow Neurological Institute ³ Ophthalmology, Neurology, and Physiology/Pharmacology, SUNY Downstate Medical Center

Corresponding Author

Stephen L. Macknik
macknik@neuralcorrelate.com

Citation

Leal-Campanario, R., Martinez-Conde, S., Macknik, S.L. In Vivo Fiber-Coupled Pre-Clinical Confocal Laser-scanning Endomicroscopy (pCLE) of Hippocampal Capillaries in Awake Mice. *J. Vis. Exp.* (194), e57220, doi:10.3791/57220 (2023).

Date Published

April 21, 2023

DOI

10.3791/57220

URL

jove.com/video/57220

Introduction

In contrast with other microscopic imaging methods^{1,2,3,4,5,6,7,8}, in vivo fiber-optic-based confocal microscopy allows the measurement of blood flow dynamics in any brain region, at any depth, at high speed (up to 240 Hz depending on field-of-view size⁹). A fiber-optic probe enables in vivo confocal laser scanning imaging at 3 μ m resolution because the tip of the probe (a lens-less objective made up

Abstract

The goal of this protocol is to describe fiber-optic-bundle-coupled pre-clinical confocal laser-scanning endomicroscopy (pCLE) in its specific application to elucidate capillary blood flow effects during seizures, driven by mural cells. In vitro and in vivo cortical imaging have shown that capillary constrictions driven by pericytes can result from functional local neural activity, as well as from drug application, in healthy animals. Here, a protocol is presented on how to use pCLE to determine the role of microvascular dynamics in neural degeneration in epilepsy, at any tissue depth (specifically in the hippocampus). We describe a head restraint technique that has been adapted to record pCLE in awake animals, to address potential side-effects of anesthetics on neural activity. Using these methods, electrophysiological and imaging recordings can be conducted over several hours in deep neural structures of the brain.

of a bundle of 5000-6000 3 μ m diameter individual fibers) can be positioned with a microelectrode's accuracy, within 15 μ m of the fluorescent target of interest. As with in vivo two-photon imaging, fluorophores must be previously introduced into the imaging target. For example, fluorescein dextran (or quantum dots) may be injected into the vasculature, or genetically-encoded fluorescent proteins can be transfected into cells,

or fluorescent dyes such as Oregon Green BAPTA-1 can be bulk-loaded into cells, prior to imaging.

Recent research using these techniques has found that mural cell motor activity leading to ictal capillary vasospasms—sudden constrictions that occur at the position of the mural cells during seizures⁹—can contribute to neurodegeneration in the ictal hippocampus⁹. Whereas previous imaging studies showed in vitro and in vivo pericyte constrictions connected to drug applications^{6,7,10,11,12}, Leal-Campanario et al. found the first evidence of in vivo spontaneous capillary constrictions in the murine brain. To establish relevance to human temporal lobe epilepsy, they studied male (P30–40 old) knockout (KO) Kv1.1 (Kcna1-null) mice^{14,15} (JAX stock #003532), a genetic model of human episodic ataxia type 1¹⁵. Pericytes drove both pathological and physiological hippocampal mural vasoconstrictions⁹ in the spontaneously epileptic animals and their wild-type (WT) littermates. These observations were replicated in WT animals rendered epileptic with kainic-acid, thereby indicating their generalization to other forms of epilepsy. Leal-Campanario et al. moreover determined, using novel stereological microscopy approaches, that apoptotic—but not healthy—neurons in epileptic animals were spatially coupled to the hippocampal microvasculature. Because excitotoxicity has no known spatial association to the vasculature, this result indicated that abnormal capillary vasospasmic ischemia-induced hypoxia contributes to neurodegeneration in epilepsy. **Figure 1** shows a schematic of the general setup.

Protocol

The protocol follows the NIH Guidelines for the Care and Use of Laboratory Animals. All procedures were approved by the

Barrow Neurological Institute's Institutional Animal Care and Use Committee.

1. Stereotaxic positioning for craniotomy

1. Weigh and then anesthetize the mouse with a ketamine-xylazine (100 mg/kg–10 mg/kg i.p.) cocktail. Ensure that the animal is fully anesthetized by observing its lack of reaction to tail and/or toe pinch.
2. Place a heating pad under the mouse and use a rectal thermometer to continuously monitor its body temperature during the initial anesthetized implantation surgery (**Figure 2A**).
3. Apply ophthalmic ointment to prevent eye dryness.
4. Stabilize the head of the animal in a rodent stereotaxic frame, outfitted with a mouse adapter. To properly orient the mouse in the stereotaxic frame, place the animal's teeth inside the hole of the bite-bar (**Figure 2A** and **Figure 3A**, item g). Tighten the nose-clamp until it is snug (**Figure 2A,B** and **Figure 3A**, item h). The mouse's body positioning should be as straight as possible (as in **Figure 2A**).
 1. Further secure the animal's head using mouse ear-bars with jaw holder cuffs (**Figure 2A** and **Figure 3A**, item i), to firmly clamp the zygomatic processes of the skull.

NOTE: Once secured, the mouse's head should have no range of horizontal motion.
5. Once the mouse is adjusted to the stereotaxic frame (**Figure 3B**, item j), clean and sterilize the scalp by wiping it with chlor-hexedine scrub 2–3 times, each time followed by an alcohol rinse. Then, apply topical lidocaine on top of the head.

6. Make an incision along the midline from posterior to anterior (start incision at the base of skull and complete it between the eyes; 12-15 mm) along the sagittal midline of the skull, using either fine scissors or a blade. Retract the borders of the scalp with four 28 mm bulldog serrefine clamps to expose the skull and maximize the working area (**Figure 2B** and **Figure 3C**).
 7. Use a scalpel or microspatula (**Figure 3C**) to scrape the periosteum to the incision's edges. Use tissue-separating scissor or forceps (**Figure 3C**) to carefully retract the muscles at the back of the neck (**Figure 2B**).
 8. Dry the top of the skull with a cotton-tipped applicator, moistened with alcohol or 30% hydrogen peroxide, to optimize visualization of the cranial sutures. Apply saline to the skull once the connective tissue has been removed.
 9. Once the mouse's head is stabilized in the stereotaxic apparatus, place a syringe needle tip (21 G) in the electrode holder (**Figure 3B**, item l), and attach the electrode holder to the stereotaxic micromanipulator, lowering the needle tip to the level of the skull (**Figure 2D**).
 10. Adjust the medial-lateral direction of the skull by measuring the height of the skull at any distance posterior to bregma (i.e., -2.0 mm), and two equal distances lateral from the midline on either side of the skull (i.e., ± 1.5 mm) (**Figure 2D**). Aim for a height difference across locations that is less than 0.05 mm in the dorsal-ventral direction.
 1. If greater than 0.05 mm, rotate the mouse's skull using the bite bar, or reposition the mouse's head by loosening the ear-bars carefully, laterally shifting the head and ear-bars as needed, and then retightening the ear-bars.
 11. Once the skull is positioned in the stereotaxic device, determine and record the stereotaxic coordinates of the bregma and lambda skull sutures along the anteroposterior (AP), medial lateral (ML), and dorsal ventral (DV) axes.
 12. Identify the target point (right hippocampus) with the aid of a stereotaxic atlas. Then, find on the skull the target point coordinates relative to bregma (AP: -2.7 mm, ML: -2.7 mm) (**Figure 2E**).
 13. Using a surgical marker, mark four corners of a 1.4 mm x 2 mm imaging window on the skull with dots, centered around the target point directly above the hippocampus (**Figure 2F**), for subsequent craniotomy.
 14. Use the surgical marker to draw two additional dots: one over the top-left parietal bone (**Figure 2G**) and another over the right frontal bone (**Figure 2H**), to indicate the future placement of two bone screws (**Figure 3A**, item b) that will anchor the head-cap (**Figure 3B**, item m) to the skull.
 15. Use the surgical marker to draw three more dots indicating where the epidural EEG recording electrodes will be inserted: one dot positioned 1 mm to either side of the midline, and one additional dot on the midline positioned 1 mm behind Lambda (**Figure 2E**, **Figure 4A** and **Figure 5B**).
- ## 2. Head-Cap installation
1. Using a 0.7 mm diameter burr (**Figure 3C**), carefully drill two small holes in the skull, at the dot positions indicating the bone screws placement (see step 1.15 above). Then, take two bone screws (stainless steel-slotted, length: 4 mm; diameter: 0.85 mm) previously disinfected with ethanol 70-80%, and screw them to the

skull for additional head-cap stability (**Figure 2I-J** and **Figure 3A**, item b).

1. Ensure that the screw tips do not protrude beyond the bottom of the bone into the skull cavity, risking damage to the brain. Note that one of the two bone screws will be anterior to the two head-cap screws, and the other posterior to them (**Figure 2G-J**).
2. Squirt saline over the skull to cool it down and clean it. Then dry the skull completely and apply a thin layer of cyanoacrylate around the screws.
3. Use a custom alignment piece (**Figure 3A**, item c) clamped to the microdrive mounted to the stereotaxic device (**Figure 2F-J** and **Figure 3A**, item d), so that the position of the head-cap is aligned along the midline, with the anterior ridge overlying bregma. This custom stainless-steel piece is L-shaped (angled at 90°), with two holes separated by 4 mm (**Figure 2F-J** and **Figure 3A**, item c).
 1. Use the stereotaxic manipulator to position the L-shaped alignment piece, with two Fillister Head Slotted drive screws attached (M1.6 x 0.35 Metric Coarse, 12 mm Length; **Figure 3A**, item a) over the bregma, until the base of the screws lies flat on the skull, being careful to not exert pressure on the skull (**Figure 2I-J**).
4. Apply cyanoacrylate followed by dental cement to attach the base of the screws to the skull. Be careful to not obstruct the imaging window reference marks over the hippocampus (**Figure 2K**).

3. Imaging window craniotomy surgery

1. At each of the positions of the craniotomy reference marks that indicate the corners of the imaging window

(see step 1.14 above), drill a 0.7 mm diameter burr hole, followed by gently delineating the periphery of the 1.4 mm x 2 mm craniotomy window with the drill, with iteratively deeper cuts (**Figure 2L**).

2. Take care to not to drill too deeply or with too much force on the skull, which is thin and fragile, having a thickness of approximately 300 µm. Once the bone flap is complete, pry the loose flap up with the tip of a scalpel, being mindful to not damage the underlying dura mater.
3. Cover the open window with bone wax (**Figure 2M**).
4. Using a 0.9 mm diameter burr, drill three holes for future placement of the epidural EEG electrodes (see step 1.15 above) taking care to not to cut through the dura mater (**Figure 2E,L**).
5. Cover the three holes with bone wax.
6. Gently apply cyanoacrylate around the edges of the bone-wax covered imaging window and EEG holes, being careful to not seal the craniotomies (**Figure 2L**).
7. Build a wall of dental cement that encompasses the imaging window and EEG holes and binds it to the previously cemented head-cap (**Figure 2M** and **Figure 3B**, item m).
8. Let the cement dry for at least 10 minutes.
9. Close any loose wound margins with simple interrupted sutures, using 4-0 or 5-0 black braided silk (**Figure 2N** and **Figure 3C**).

4. Post-surgery

1. Use a cotton-tipped applicator to apply lidocaine ointment around the exposed skin to deaden sensation around the wound's edge.

2. Use a sterile cotton-tipped applicator to apply Neosporin to the exposed skin.
 3. Remove the animal from the stereotaxic frame (**Figure 2N**).
 4. Inject ketoprofen (5 mg/kg) IP or IM for post-surgical analgesia.
 5. Observe the animal until it is alert and moving (this will usually occur within minutes).
 6. Place the animal in a warm cage and continue to monitor its recovery until it drinks or eats and is ready to transfer to animal housing.
 7. Check on the animal at least once daily for approximately one week after the surgery, watching for any signs of listless behavior and/or inadequate eating/drinking (**Figure 2O**).
4. Insert the epidural EEG recording electrodes (**Figure 5A**), placing the ground electrodes (white wires) within the posterior central hole, and the recording electrodes (red wires) in the anterior left and right holes (**Figure 2E**, **Figure 4E** and **Figure 5E**). Position each of the wires at an L-shape between the skull and the dura mater (**Figure 5C**) to optimize electrical contact.
 5. Inject the tail vein with green fluorescein lysine-fixable dextran (0.2 mL/25 g body wt. of Fluorescein 5% w/w), to visualize blood flow within the hippocampus.
 1. To enhance dilation of the central vein of the mouse's tail previous to injection, use one or more of the following strategies: a) Apply 70% ethanol to the central vein using a cotton-tipped applicator; b) Dip the tail into warm water (35-40 °C) for 1-3 minutes; c) Expose the tail to a heating lamp for a few minutes.

5. Dye injection and EEG recording

1. Wait a minimum of one day after the head-cap implantation surgery to initiate the recordings.
 2. Place the mouse in a foam-restraining device molded to its body, within the stereotaxic frame (**Figure 3B**, items n & j).
 3. Secure the head-cap (**Figure 3B-I**, item m) to a custom mounting bar which is attached to the stereotaxic frame (**Figure 3A,B**, items e & j, and **Figure 4A**). The long section of item e (**Figure 3A,B**) should have a length between 9.4 – 13 mm. Fix item f (a mounting plate with dimensions 1.5 cm x 0.5 cm, with two holes separated 4 mm from center to center) to item e (**Figure 3A,B**, items e, f and k). This alignment system will position the awake mouse securely to the stereotaxic frame throughout the imaging sessions (**Figure 4**).
2. Secure the mouse's tail with two fingers and locate the central vein, which lies immediately below the skin. Insert the needle (ultrafine insulin syringe with integrated needle 30G), with the bevel up, into the vein, approximately halfway to two thirds from the base of the tail. Keep the needle parallel to the tail during the injection.
 3. Inject the dye slowly and steadily, taking care to avoid any changes in the position of the needle or tail.

NOTE: There should be no resistance upon depressing the syringe plunger.
 4. After completing the injection, withdraw the needle and apply gentle pressure to the puncture site to seal the vessel.
 5. Allow clotting to occur.

6. In vivo fiber-optic-bundle-coupled pre-clinical confocal laser-scanning endomicroscopy (pCLE)

1. Directly following the tail vein injection (step 5.5.3 above), clamp the 300 μm beveled fiber-optic bundle (containing 5000–7000 3 μm fibers in each bundle) in the downward orientation to the mobile arm of the robotic stereotaxic drive.
2. Remove the bone wax from the craniotomy.
3. Remove the dura, using the bent tip of a syringe needle.
4. Using the robotic positioning system, first move the fiber objective to the appropriate anterior-posterior and left-right stereotaxic location, with the tip zeroed in the z-axis on the surface of the cortex.
5. Initiate the EEG recording (**Figure 5D**).
6. Initiate confocal laser-scanning of the back plane of the fiber-objective, followed directly by descending the objective slowly in the z-axis using the robotic microdrive's z-controls, until it reaches the target depth within the brain (**Figure 4C**). View the imaging results in the microscopic software while descending.
 1. If the fiber tip is within the target X-Y-Z recording region, and two or more vessels enter the imaging window's FOV, stop the descent and initiate video recordings. Obtain live full-field time-lapse movies of the blood flow at 11.7 Hz using Cellvizio Lab's imaging software. (Higher speeds may be obtained with a smaller FOV). Recordings may take place for 4-5 hours at a time, in consecutive days if needed.
7. Using a 10 mL syringe with beveled silicon tubing fixed to the tip of the needle, feed the animal during the recordings by periodically providing paste made with mice pellets ground with water.

8. At the end of the imaging session, terminate the recordings.
9. Gently remove the EEG leads and clean them with Tergazyme.
10. Slowly remove the fiber-optic bundle from the animal's brain by reversing the fiber along the z-axis of entry.
11. Release the animal from the head post and body restraints.
12. If appropriate, follow the necessary euthanasia and tissue processing protocols to visualize blood vessels and to perform immunohistochemistry.
13. If planning to record from the same animal in a future session, cover the imaging window with bone wax or silastic.

Representative Results

We developed these methods to assess whether abnormal pericyte-driven capillary vasospasms in the hippocampus—occurring as the result of seizures—could cause frank hypoxia that contributes to cell death in the ictal focus^{9,13}.

The development of the head-cap and its proper installation afforded high-stability in the recordings, allowing simultaneous recording of EEG and blood flow deep in the hippocampus of wild-type and epileptic awake mice during both ictal and interictal periods. Capture of blood flow events related to seizures requires recording for extended periods of time, so that aperiodic blood flow events (such as vasospasms) can be captured in response to both induced and naturally occurring epileptic seizures. The restraint system permitted stable blood flow recordings of deep brain microvessels and their proximal mural cells over long hours (**Figure 6A-R**). We found that, in entire microvessels, blood

flow stoppages occurred at the positions of labelled mural cells.

We reliably located vessels in the hippocampus using a robotic stereotaxic device targeted with internal coordinates from a standard stereotaxic atlas. We verified the quality of the fiber recordings by comparing them to high-resolution two-photon imaging recordings of blood flow and equivalent vasospasms from cortical tissue, at depths that two-photon imaging can reach (**Figure 6S-AA**). We further verified the pCLE results using immunohistochemistry at recording sites, to show with traditional confocal microscopy that hippocampal

mural cells were targeted correctly and that they were not only constricting but also spatially associated with strictures in microvessels far from arterioles¹⁵ (**Figure 7**).

The published findings with these methods indeed show abnormal hippocampal capillary vasospasms driven by seizures, as well as correlated cell death in Kv1.1 epileptic mutant mice and kainate model epileptic mice^{9,13}. These results indicate a role for local ictal ischemia/hypoxia in cell death during seizures, due to abnormal vasospasms, and contribute to a growing body of work that expands on the potential mechanisms of ictal cell death.

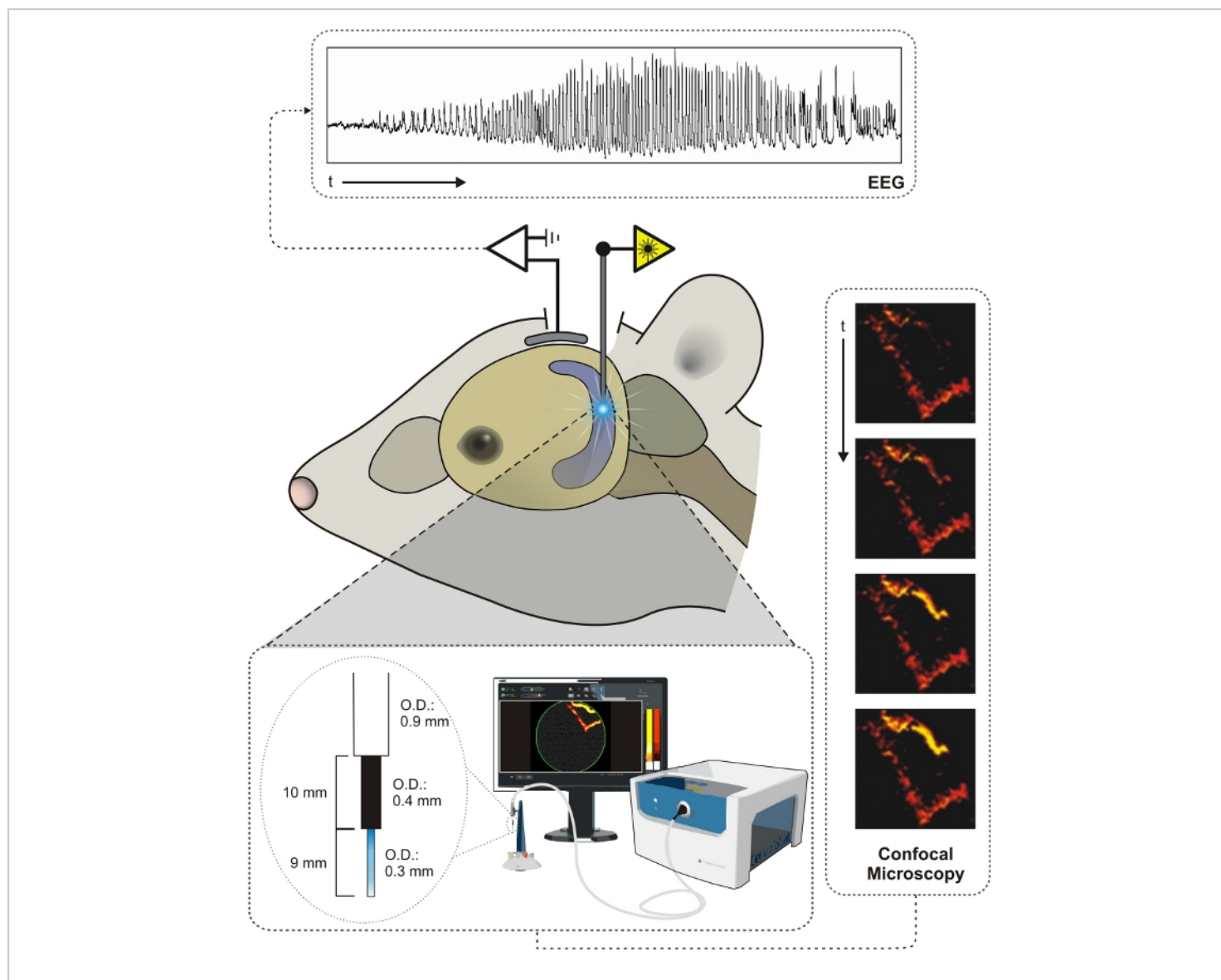


Figure 1: Schematic representation of the experimental design. We recorded EEG while conducting confocal microscopy in hippocampal capillaries of both awake epileptic mice and WT littermates. After injecting the tail vein with fluorescein, we used a novel preclinical Confocal Laser-scanning Endomicroscopy (pCLE), with a fiber-objective with a tip diameter of 0.3 mm to record capillary blood flow dynamics deep in the brain. Yellow indicates increased blood flow, and red indicates steady or reduced flow. [Please click here to view a larger version of this figure.](#)

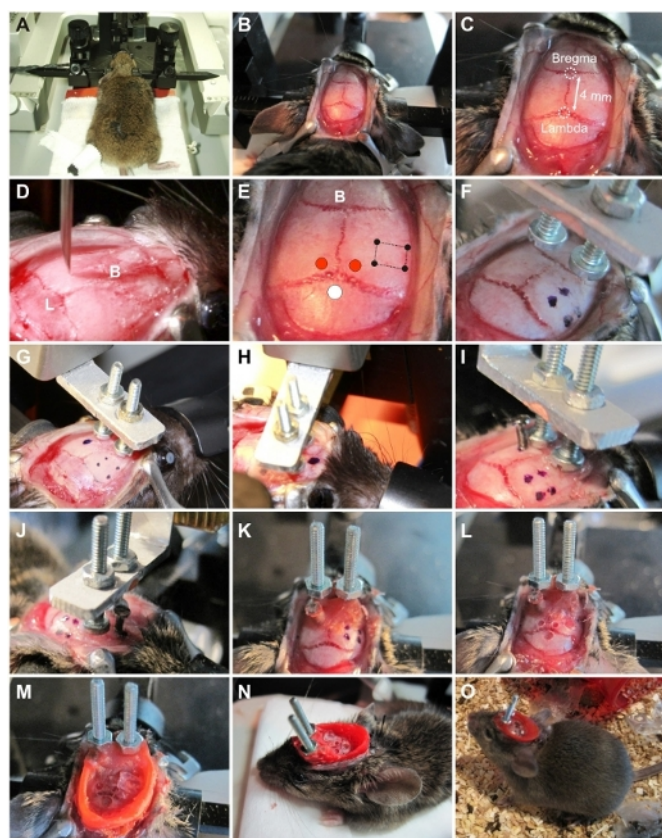


Figure 2: Protocol for head-cap implantation surgery. **A)** The anesthetized animal was placed on a heating pad and positioned within the stereotaxic frame (see **Figure 3B**, item j) and secured with mouse ear-bars (**Figure 3A**, item i) and jaw holder cuffs (**Figure 3A**, items g,h), over a heating pad. **B)** Exposure of the cranial sutures. **C-D)** Measurements of Bregma and Lambda. **E)** Visualization of drilling locations over the animal's skull. The black points and square indicate the window over the hippocampus that will permit the pCLE insertion. The two red circles mark the insertion positions for the EEG recording wires. The white dot marks the insertion point of the EEG ground wires. **F)** The four black dots on the skull mark the future corners of the imaging window craniotomy over the hippocampus. The custom alignment piece (**Figure 3A**, item c), with the headpost implants (**Figure 3A**, item a) attached to the stereotactic microdrive positioner (**Figure 3A**, item d). **G-H)** Two additional dots, one posterior (**G**) and one anterior (**H**) mark the future location of head-cap anchor screws (**Figure 3A**, item b). **I-J)** Two small screws anchor the head-cap to the skull (**Figure 3A**, item b). **K)** Cyanoacrylate and dental cement are applied to the anchor screws from panels I & J. **L)** The imaging window craniotomy over the hippocampus, and the three holes for the EEG electrodes, have been drilled. **M)** The imaging chamber is built (**Figure 3B**, items i, m) by sculpting a berm with additional dental cement to encircle the three EEG holes and the imaging window. **N)** Overhead view of the finished head-cap. **O)** The recovered mouse back in its cage after the implantation surgery. [Please click here to view a larger version of this figure.](#)

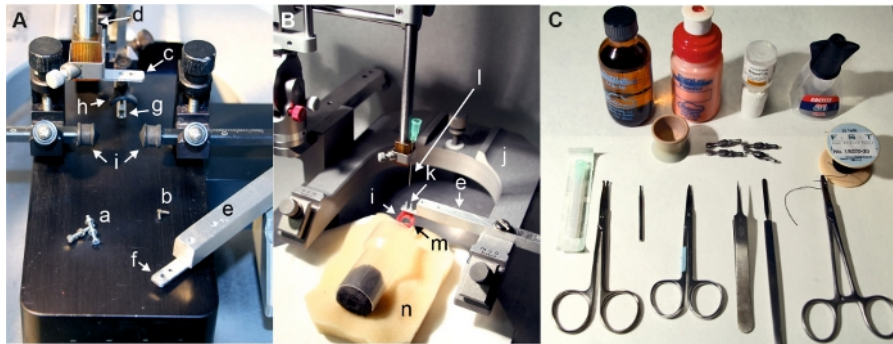


Figure 3: Materials used in the Protocol (specific items enumerated with lower-case letters). **A)** Materials used to build the head-cap. **(a)** Two M1.6 x 12 mm machine screws (the headpost implants). **(b)** Two small bolts to secure the head-cap to the skull. **(c)** A custom L-shaped stainless-steel alignment piece, with two holes 4 mm apart, which secures the two M1.6 screws during the surgery. **(d)** A standard microdrive mounted on a stereotaxic device holds item c. **(e)** A custom mounting bar with an **(f)** alignment piece that matches the two holes from item c. **(g)** A bite bar and **(h)** nose clamp to stabilize the position of the animal's head. **B)** Setup during the recordings. **(i)** The head-cap is secured to item f during the anesthetized implantation surgery. **(j)** A stereotaxic frame positions the microdrive (item d). **(l)** A 21G needle is attached to the microdrive (item d) and used to determine the positions of the Bregma and Lambda cranial sutures. **(m)** A simulated head-cap is pictured here, attached to item f, to demonstrate the positioning of the mouse in **(n)** the foam-lined restraining-tube (mouse not present). Item n molds itself to the shape of the mouse's body. **C)** Instruments and supplies needed to perform the surgery. [Please click here to view a larger version of this figure.](#)

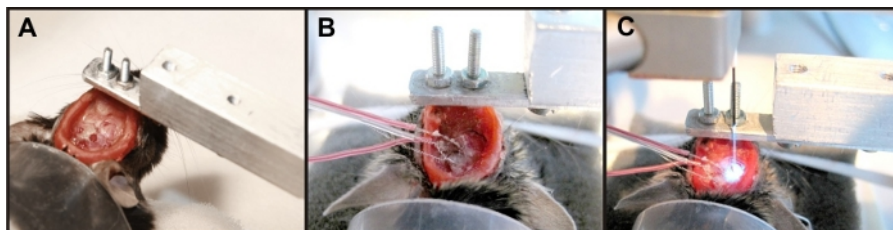


Figure 4: Recording session setup. **A)** The animal's head is fixed. **B)** Location of the EEG recording wires. White EEG wires are placed separately, in each side of the skull. Red EEG wires are placed together in the middle-bottom (ground) hole. **C)** The fiber-optic bundle is inserted into the target window. [Please click here to view a larger version of this figure.](#)

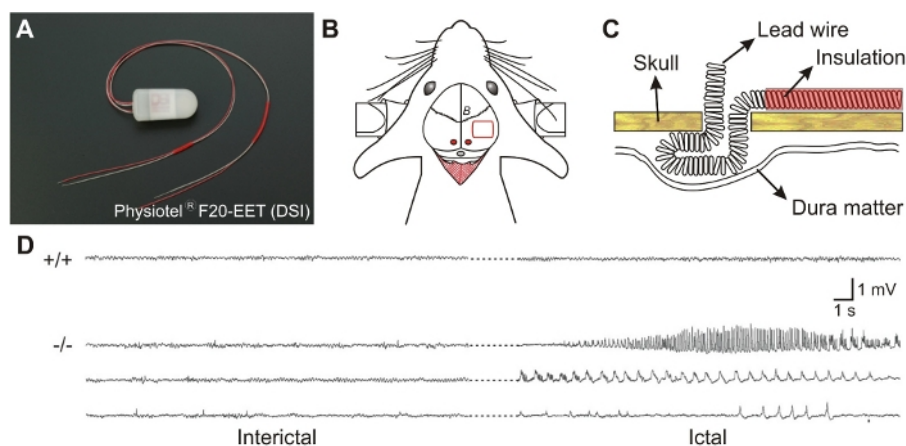


Figure 5: EEG recordings. **A)** Epidural EEG recordings are conducted with Physiotel F20-EET transmitters, simultaneously to the fiber-optic pCLE recordings in the awake animal. **B)** Location of the drilled holes for insertion of the leads for EEG recordings. The two red leads go to the two holes indicated by red dots. The two white leads are inserted together in the hole indicated by the white dot. The red square designates the target window over the animal's hippocampus. The letter 'B' on the mouse's skull indicates the bregma. **C)** The EEG recording wires are bent in an L-shape to enhance electrical contact between the skull and the dura matter. **D)** Examples of EEG recordings in awake mice. [Please click here to view a larger version of this figure.](#)

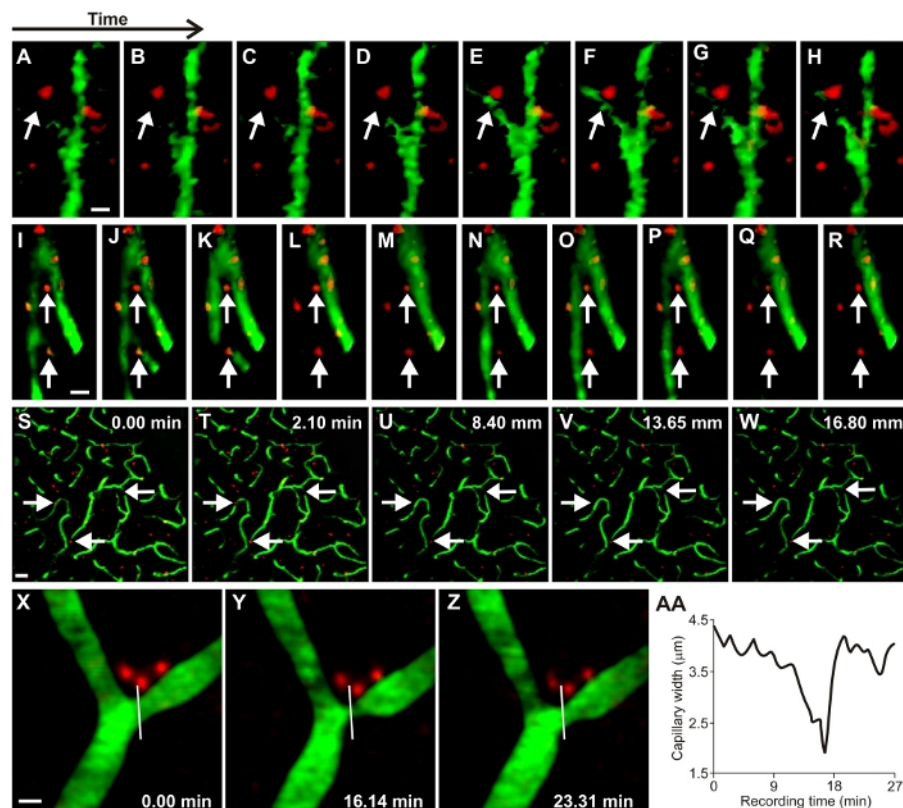


Figure 6: Recordings of mural cell vasoconstrictions in mice. **A-R)** In vivo fiber-optic dual-band pCLE image of capillary vasospasm (vessels in green, labeled with 2MD fluorescein-conjugated dextran) colocalized to mural cells (red, labeled via intravenous vein tail injection of Alexa Fluor 647) in awake knockout mice during seizure (arrow indicates mural cell and associated vasospasm). See **Video 1** and **Video 2**. **S-W)** In vivo two-photon scanning laser microscopy (TPLSM) stack of capillary vessels (green) and mural cells (red) of a wild type mouse. See **Video 3**. **X-Z)** In vivo TPLSM of a mural-cell-localized (red) capillary constriction of kainic mice. See **Video 4**. **AA)** Quantification of vessel constriction from panels X-Z measured at white line. Scales for panels A-R= 5 μm ; S-W= 25 μm ; X-Z= 5 μm . Videos were recorded at 11.7 Hz. From Leal-Campanario et al.⁸. [Please click here to view a larger version of this figure.](#)

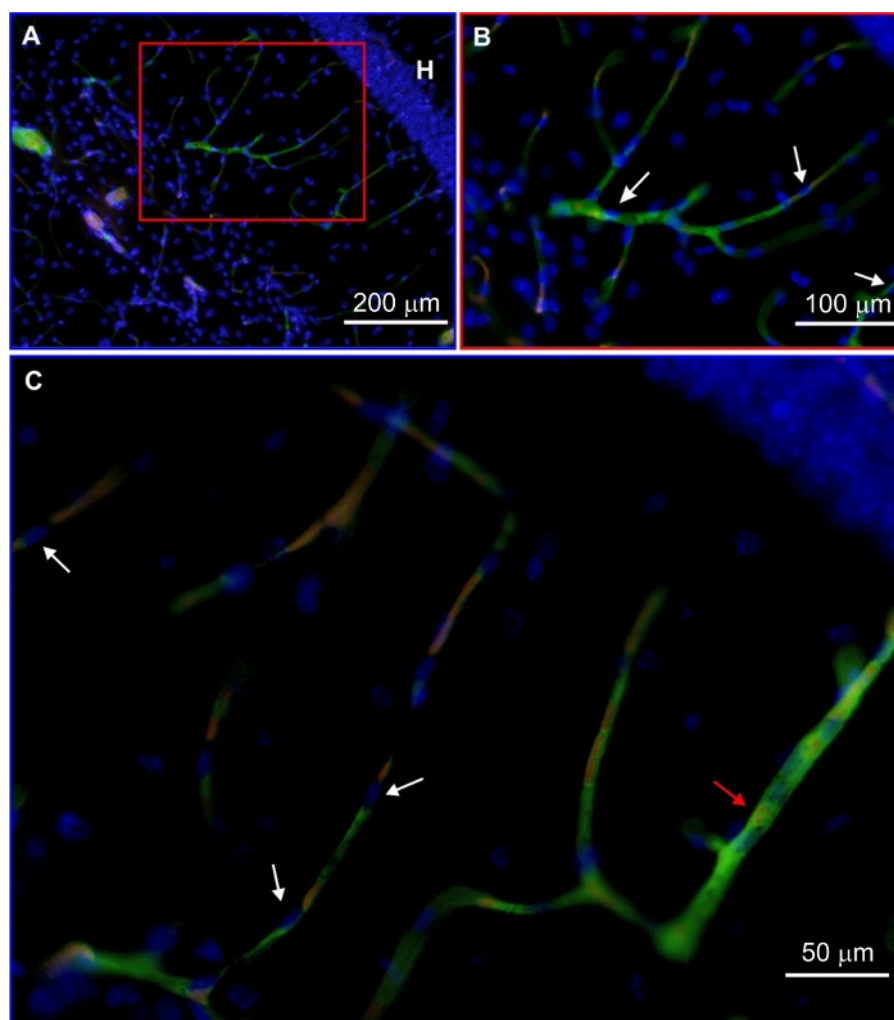


Figure 7: Immunohistochemistry of the recorded brain. A-B) Vessels at different magnifications injected with fluorescein dextran (green). DAPI-stained cellular nuclei in blue (white arrows). Scale bar for A= 200 μm ; scale bar for B = 100 μm . **C)** Different section of the brain injected with fluorescein where a red blood cell (red arrow) is clearly seen. Scale bar = 50 μm .

[Please click here to view a larger version of this figure.](#)

Video 1: Vasospasm and mural cell blood flow recorded (11.7 Hz) in a KO hippocampal capillary. See frames from the same recording in **Figure 6A-H**. [Please click here to download this video.](#)

Video 2: Vasospasm, leukocyte blockages, blood flow and mural cells recorded in a WT hippocampal capillary (11.7 Hz).

See frames from the same recording in **Figure 6I-R**. [Please click here to download this video.](#)

Video 3: Non-uniform blood flow in in vivo WT mouse parietal cortex recorded with TPLSM. See frames from the same recording in **Figure 6S-W**. [Please click here to download this video.](#)

Video 4: Mural cell-driven (red) capillary (green) constriction from parietal cortex of seizing kainic animal recorded with TPLSM. See frames from the same recording **Figure 6X-Z**.

[Please click here to download this video.](#)

Discussion

We developed a head-cap restraint system for simultaneous electrophysiological and fiber-optic pCLE experiments in awake mice, reducing potential response contamination due to anesthetic drugs. The head-cap and mounting apparatus are straightforward to construct and are reusable for chronic awake-behaving imaging experiments. We checked the quality of the recordings against the gold-standard for in vivo microscopic blood flow imaging, TPLSM.

Proficient surgical skills are necessary to implement the protocol we describe here. The surgery must be done under aseptic conditions and always under an operating microscope, while taking care to leave the dura mater intact when drilling the window over the hippocampus. Familiarity with the underlying vasculature is essential, as cutting above a major blood vessel creates the risk of undesirable bleeding.

Placing the animal correctly in stereotaxic alignment ensures that the anterior-posterior plane is level before attaching the head-cap. This safeguard facilitates locating brain loci with the help of a brain atlas.

Mouse motion can result in damage to vessels or erroneous recordings of vasospasms (that is, fiber motion rather than true vasomotion), so it is important to reduce animal motion during the recordings. Foam padding within the restraint tube helps extend the duration of the recording sessions while minimizing stress and movement from the mouse. Mice prefer to fit snugly within the foam, so proper fitting reduces excessive motion. Without this precaution, mice may struggle.

If the mouse does show signs of struggle, the recording session should be terminated. Recordings may resume the next day, once physiological stress reactions have abated. In our recordings, the animals were evidently calm most of the time.

We note that the motion that most negatively impacts the pCLE imaging method occurs when the probe moves differentially to the brain tissue. Breathing, seizures, and motion of the animal are irrelevant unless they displace the fiber-probe with respect to the tissue. That is, when the imaging probe moves differentially to the tissue the entire imaging field moves as a unit, making motion artifacts evident. Thus, it is critical to always record from two or more vessels at a time: if all vessels move at once, it may be due to fiber instability, whereas if at least one vessel does not change, the changes seen in other vessels are likely due to actual variations in blood flow, including vasospasms.

One limitation of the pCLE imaging method compared to TPLSM is that the fiber-probe punctures the pia and is thus invasive to the brain. As the probe descends, it causes some damage to the neural tissue it passes through. Thus, recording from the same vessel on two consecutive days can be exceedingly difficult, even when employing the same exact coordinates in both sessions (and often only possible if the initial recording session has a short duration). It is therefore critical, when conducting chronic recording studies, to record at increasingly greater depths in subsequent recording sessions.

The results of the blood flow experiments suggest that excitotoxicity is not the only mechanistic pathway for ictal cell death and hippocampal sclerosis¹³. The finding that capillary blood flow restriction plays a role in ictal neurodegeneration paves the way for extending the methods described here to

the identification of microscopic blood flow changes at any depth of the body, and in any tissue, for clinical diagnostic purposes.

Disclosures

We have nothing to disclose.

Acknowledgments

The project was funded by a Research Initiative Award from the American Epilepsy Society, and an award from the Arizona Biomedical Research Commission to S.L.M., as well as a challenge grant from Research to Prevent Blindness Inc. to the Department of Ophthalmology at SUNY Downstate Health Sciences University, the New York State Empire Innovation Program, and further grants from the National Science Foundation (0726113, 0852636, & 1523614), the Barrow Neurological Foundation, Mrs. Marian Rochelle, Mrs. Grace Welton, and Dignity Health SEED awards, and by federal grants from the National Science Foundation (0726113, 0852636, & 1523614) and by the National Institute of Health (Awards R01EY031971 AND R01CA258021), to S.L.M and S.M.C. This work was also supported by the Office of the Assistant Secretary of Defense for Health Affairs under Award No. W81XWH-15-1-0138, to S.L.M.. L.-C. was supported by a José Castillejo fellowship from the Spanish Ministry of Education. We thank O. Caballero and M. Ledo for their technical advice and assistance.

References

1. Denk, W. et al. Anatomical and functional imaging of neurons using 2-photon laser scanning microscopy. *Journal of Neuroscience Methods*. **54** (2), 151-62 (1994).
2. Kleinfeld, D., Mitra, P.P., Helmchen, F., Denk, W. Fluctuations and stimulus-induced changes in blood flow observed in individual capillaries in layers 2 through 4 of rat neocortex. *Proceedings of the National Academy of Sciences of the United States of America*. **95**, 15741-15746 (1998).
3. Helmchen, F., Fee, M. S., Tank, D. W., Denk, W. A miniature head-mounted two-photon microscope. High-resolution brain imaging in freely moving animals. *Neuron*. **31**, 903-9012 (2001).
4. Chaigneau, E., Oheim, M., Audinat, E., Charpak, S. Two-photon imaging of capillary blood flow in olfactory bulb glomeruli. *Proceedings of the National Academy of Sciences of the United States of America*. **100**, 13081-13086 (2003).
5. Larson, D.R. et al. Water-soluble quantum dots for multiphoton fluorescence imaging in vivo. *Science*. **300**, 1434-1436 (2003).
6. Hirase, H., Creso, J., Singleton, M., Bartho, P., Buzsaki, G. Two-photon imaging of brain pericytes in vivo using dextran-conjugated dyes. *Glia*. **46**, 95-100 (2004).
7. Hirase, H., Creso, J., Buzsaki, G. Capillary level imaging of local cerebral blood flow in bicuculline-induced epileptic foci. *Neuroscience*. **128**, 209-216 (2004).
8. Schaffer, C.B. et al. Two-photon imaging of cortical surface microvessels reveals a robust redistribution in blood flow after vascular occlusion. *PLoS Biology*. **4**, e22 (2006).
9. Leal-Campanario, R. et al. Abnormal Capillary Vasodynamics Contribute to Ictal Neurodegeneration in Epilepsy. *Scientific Reports*. **7**, 43276 (2017).
10. Peppiatt, C.M., Howarth, C., Mobbs, P., Attwell, D. Bidirectional control of CNS capillary diameter by pericytes. *Nature*. **443**, 700-704 (2006).

11. Yemisci, M. et al. Pericyte contraction induced by oxidative-nitrative stress impairs capillary reflow despite successful opening of an occluded cerebral artery. *Nature Medicine*. **15**, 1031-1037 (2009).
12. Fernandez-Klett, F., Offenhauser, N., Dirnagl, U., Priller, J., Lindauer, U. Pericytes in capillaries are contractile in vivo, but arterioles mediate functional hyperemia in the mouse brain. *Proceedings of the National Academy of Sciences of the United States of America*. **107**, 22290-22295 (2010).
13. Leal-Campanario, R., Alarcon-Martinez, L., Martinez-Conde, S., Calhoun, M., Macknik, S. Blood Flow Analysis in Epilepsy Using a Novel Stereological Approach. *Neurostereology: Unbiased Stereology of Neural Systems*. ed Mouton PR John Wiley & Sons, Inc., Ames, USA (2013).
14. Smart, S.L. et al. Deletion of the K(V)1.1 potassium channel causes epilepsy in mice. *Neuron*. **20**, 809-819 (1998).
15. Zuberi, S.M. et al. A novel mutation in the human voltage-gated potassium channel gene (Kv1.1) associates with episodic ataxia type 1 and sometimes with partial epilepsy. *Brain*. **122**, 817-825 (1999).